Hindawi
Shock and Vibration
Volume 2020, Article ID 3835015, 18 pages
https://doi.org/10.1155/2020/3835015

Research Article

Response Modification Factor of RC Frames Strengthened with RC Haunches

Junaid Akbar, Naveed Ahmad, Muhammad Rizwan, Sairash Javed, and Bashir Alam

Earthquake Engineering Center, UET Peshawar, Peshawar, Pakistan

Correspondence should be addressed to Naveed Ahmad; naveed.ahmad@uetpeshawar.edu.pk

Received 3 September 2019; Revised 30 November 2019; Accepted 15 June 2020; Published 7 July 2020

Academic Editor: Fabio Rizzo

This paper presents experimental and numerical studies carried out on two-story reinforced concrete (RC) frames having weaker beam-column joints, which were retrofitted with reinforced concrete haunches to avoid joint panel damage under seismic actions. The design philosophy of the retrofit solution is to allow beam-column members to deform inelastically and dissipate seismic energy. Shake table tests were performed on three 1 : 3 reduced scale two-story RC frame models, including one model incorporating construction deficiencies common in developing countries, which was retrofitted with two retrofit schemes using RC haunches. The focus of the experimental study was to understand the seismic behaviour of both as-built and retrofitted models and obtain the seismic response properties, i.e., lateral force-displacement capacity curves and time histories of model response displacement. The derived capacity curves were used to quantify overstrength and ductility factors of both as-built and retrofitted frames. Finite element- (FE-) based software SeismoStruct was used to develop representative numerical models, which were calibrated with the experimental data in simulating the time history response of structure roof displacement and in predicting peak roof-displacement and peak base shear force. Moreover, the FE-based numerical models were subjected to a suite of spectrum natural accelerograms, linearly scaled to multiple intensity levels for performing incremental dynamic analysis. Lateral force-displacement capacity and response curves were developed, which were analyzed to calculate the structure ductility and overstrength factors. The structure R factor is the product of ductility and overstrength factors, which exhibited substantial increase due to the proposed retrofitting technique. A case study was presented for the seismic performance assessment of RC frames with/without RC haunches in various seismic zones using the static force procedure given in seismic code and using response modification factor quantified in the present research.

1. Introduction

Non-seismic design or poorly built RC frames have exhibited significant vulnerability in recent earthquakes, and in experimental tests, against seismic actions [1–14]. RC frames having lower concrete strength, improper reinforcement detailing, and beam-column joints lacking ties have experienced joint damage under lateral loads that have resulted in brittle shear hinging at local level and soft-story mechanism at global level [15–21]. Various more or less sophisticated strengthening and isolation techniques have been investigated for seismic performance improvement of structures [22–31]; however, a low-cost and less invasive haunch retrofitting *technique* for structures has *exhibited* better seismic performance under seismic induced strong vibrations [32–35]. Despite the recent work on haunch retrofitting technique, there is still lack of significant amount of data to help the structural engineers design or validate haunch-retrofitted structures using static force procedure given in national seismic codes. One such piece of information required is the response modification factor R, essential for structural design and assessment in various seismic zones.

2. Description of Test Frame Models

Static force-based procedure was used for seismic analysis of a two-story special moment resisting frame (SMRF) structure for a design base shear of 0.12 W, where W is the seismic weight of the structure. The design was carried out for SMRF

structure located in a seismic zone 4 on rock site "type B soil," with design base ground motion of 0.40 g and response modification factor $R = 8.50$. Concrete with compressive strength of 3000 psi (20.68 MPa) and Grade 60 rebars with yield strength of 60,000 psi (414 MPa) and ultimate strength of 90,000 psi (621 MPa) were considered for analysis and design. Beams and columns were designed for seismic actions using the seismic design provisions of ACI 318-05 [36] for SMRF. Such design is commonly practiced in Pakistan in areas with high to very high seismic hazard. However, execution of constructions as per the specification in the field still remains a challenge in most of the developing countries; hence, significant building stock can be found in these countries possessing construction deficiencies like lower strength of concrete, low quality and reduced size rebars, reduction in the longitudinal and transverse reinforcement, poor anchorage details, and beam-column joints lacking confining ties.

Therefore, the present study considered two typologies of deficient frames: a noncompliant SMRF Model-M_{RC} and Model-M_{RC2}. The first model Model-M_{RC} incorporated deficiencies like lower concrete strength, beam-column joints lacking confining ties, and beam/column members having reduced longitudinal and transverse reinforcement. This model was retrofitted with RC haunches applied below the beam. The second model Model-M_{RC2} incorporated similar construction deficiencies, which was retrofitted with RC haunches applied both below and above the beam. Figure 1 shows the details of the RC frame, which was considered for retrofitting using RC haunches, and experimental and numerical investigations.

2.1. Design of Haunch Retrofit for RC Frames. The installation of haunch stiffens the beam-column connection and shifts the inelastic hinge in beam at distance from the beam-column interface and consequently reduces shear stress demand on the beam-column joint (Figure 2). The proposed analytical formulation of Pampanin et al. [33] was used for the preliminary design of haunches, which were verified through nonlinear finite element based analysis of beam-column assemblages.

Figure 3 shows the geometric details and pictorial view of the designed RC haunches for 1 : 3 reduced scale test frame. RC haunches consisted of 6#2 bars provided in diagonal pattern. Fabrication of RC haunches involved cutting steel bars to desired length and then bending them to L shape. Holes were drilled in beam and column distributed over 1 h length, where h is the depth of beam/column depth. The required rebars were inserted in epoxy-filled holes. The SIKA Latex *R* grout, meeting the requirements of ASTM C-882, was used as bonding agent to develop bond between anchors and concrete. One end of rebars was embedded and anchored in column while the other end was embedded in beam. The minimum requirement for development length of rebars was satisfied to ensure the rebars remain intact during closing/opening of connections. Experimental pullout tests conducted on embedded rebars in concrete cylinders with similar epoxy suggested the minimum embedded length of 6 inches (152.40 mm) in prototype that reduced to 2 inches (50 mm) in test model. The development length requirement of rebars was based on the actual pullout tests. The rebar insertion followed pouring of concrete in a special fabricated formwork. The haunches were cured for 28 days to attain their desired strength. Figure 4 shows the RC haunch retrofitted schemes investigated in the present research.

3. Shake Table Testing of RC Haunch Retrofitted Frames

3.1. Preparation of the Test Models. A 1 : 3 reduced scale simple idealization was adopted to prepare shake table test models. This considers only geometric scaling of beam/column member dimensions and diameter of steel rebars. All the linear dimensions were reduced by a scale factor of $S_L = 3$. Concrete having mix ratio of 1 : 3.50 : 2.87 (cement: sand: aggregate) with water-to-cement ratio of 0.80 was used to prepare the test model. The mix was used to simulate the field condition found in recent constructions in Pakistan. The test models were provisioned with additional floor masses as suggested [37] to simulate the required static stress and dynamic mass for a 1 : 3 reduced scale model. Additional floor mass of 1200 kg was provided on each floor by mounting steel blocks of 600 kg on each side of beam, which was firmly secured by means of anchor bolts. Figure 5 shows the final prepared model mounted on the shake table. The test model was instrumented with five displacement transducers and accelerometers to record the time histories of response acceleration and displacement at floor levels and base of the model. Two instruments were installed at each floor for averaging the floor response.

3.2. Acceleration Time History for Input Excitation. The 1994 Northridge earthquake acceleration time history recorded at the 090 CDMG Station 24278, which was obtained from the PEER strong motion database, was selected for input excitation of the test model (Figure 6). This time history has a maximum velocity of 518 mm/sec, maximum displacement of 90 mm, and a maximum acceleration of 0.57 g. The acceleration time history was linearly scaled to multiple intensity levels, i.e., 5%, 10%, 20%, 30%, 40%, 50%, 60%, 70%, 80%, 90%, and 100% of maximum acceleration of the record. The model was tested incrementally from low to high input excitation till the model reached the incipient collapse state. The observed damage of model was recorded after each test run.

3.3. Observed Seismic Behaviour of Haunch Retrofitted RC Frames. In comparison to the as-built models tested by Rizwan et al. [19], the application of RC haunches at the beam-column connection altered the initial damage mechanism. Flexure cracks were observed in beams and columns at distance from the beam-column interface, which were distributed over significant length (Figure 7). In case of Model-M_{RC}, slight vertical cracks were noted at the haunch-column interface of ground-story columns, indicating haunch rebars slip and pullout. Diagonal cracks also

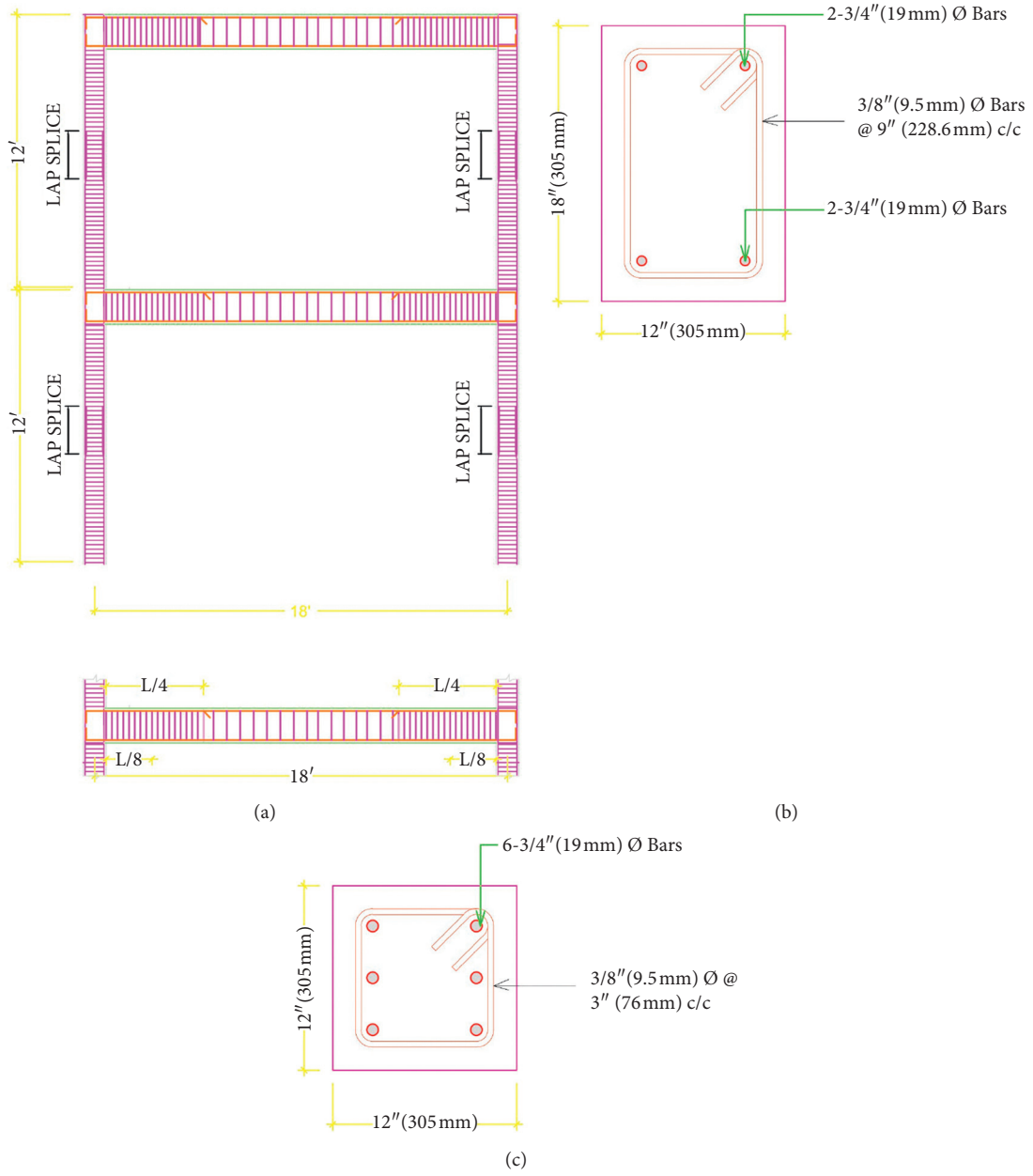

Figure 1: Geometric and reinforcement details of the considered RC SMRF structure. (a) Beam long section. (b) Beam cross section. (c) Column cross section.

appeared in columns on the outer side behind the haunches on both the ground-story and top-story, which was due to haunch strut action. It is worth to mention that the joint panel did not receive any crack throughout the loading. In case of Model-M_{RC2}, minor flexure cracks were observed in ground-story columns at the top ends. Substantial horizontal and vertical cracks were also observed in haunch at the beam-haunch and column-hunch interfaces, respectively. Propagation of significant vertical and diagonal cracks was observed also at the ends of first-floor beam due to haunch strut action. Only slight cracks were observed in beam-column joint panel under extreme shaking, because of the pullout of haunch rebars from beam.

Figure 8 shows the extent of damage observed in beam/column members and beam-column joints upon subjecting the model to extreme level shaking. Such damage was relatively more severe in model where haunches were applied only below the beam, because the strain in the longitudinal rebars of columns at the bottom ends penetrates through the joints under tension load that results in stress demand on panel zone. The shaking induced stress demand in joint panel can result in joint damage upon exceeding the joint principal tensile strength [16, 17, 38]. This was creating a hinge at the base of column, likely to promote soft-story mechanism. It can be observed that the application of haunch applied either below or both below and above the

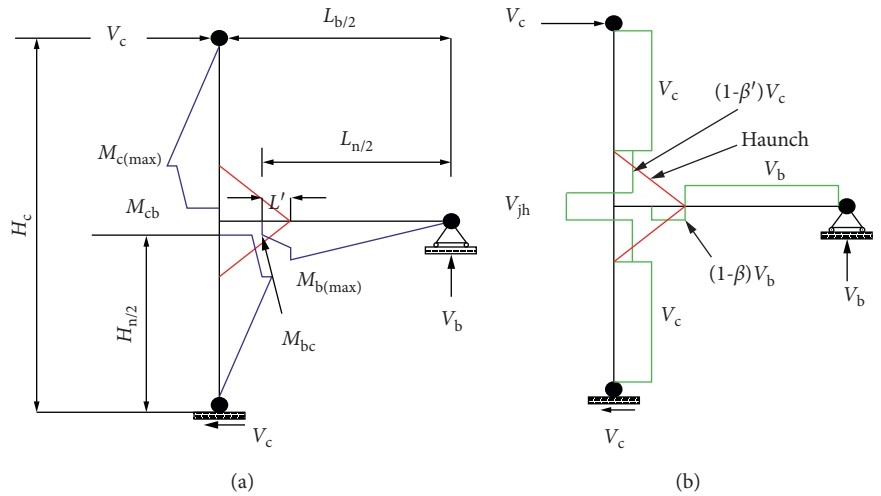

FIGURE 2: Modified bending moment and shear actions in a haunch retrofitted beam-column sub-assemblages under lateral load. (a) Bending moment diagram. (b) Shear force diagram.

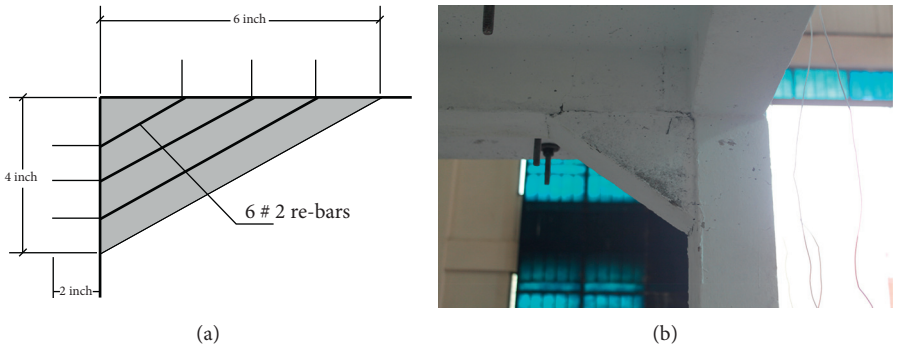

FIGURE 3: Geometric and reinforcement details of RC haunches for 1 : 3 reduced scale models. (a) Details of RC haunch (1 : 3 scale). (b) Pictorial view of the model haunch.

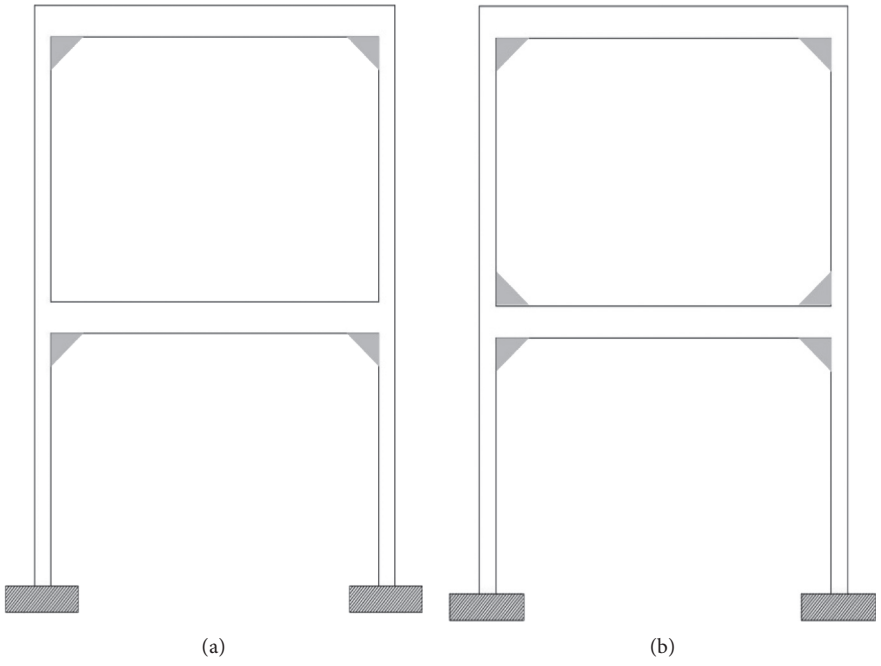

FIGURE 4: RC haunch retrofitting schemes considered for investigation in the research [33]. (a) Model-MRC RC haunch below beam only. (b) Model-MRC2 RC haunch both below and above beam.

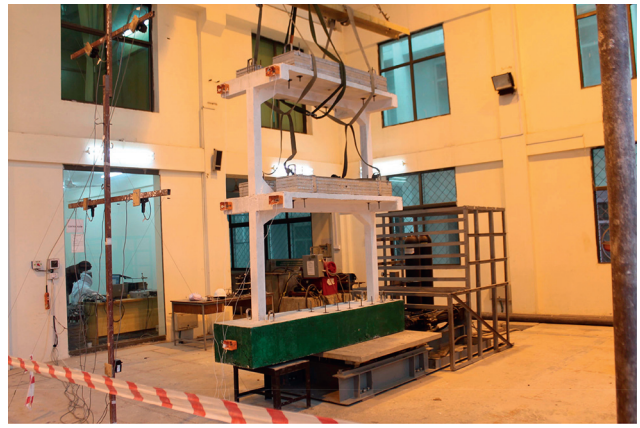

Figure 5: 1 : 3 reduced scale model prepared for shake table testing.

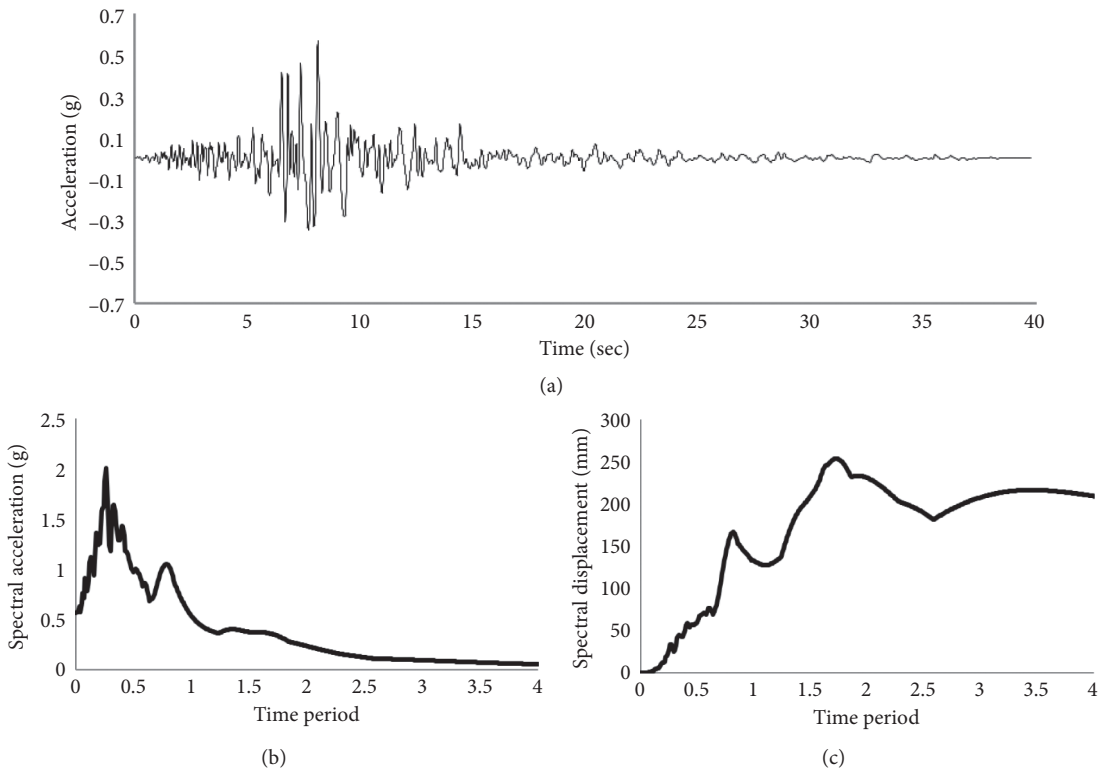

Figure 6: Natural accelerogram of 1994 Northridge earthquake used for shake table testing. (a) Northridge 1994 acceleration time history. (b) 5% damped acceleration response spectra. (c) 5% damped displacement response spectra.

beam can avoid joint cracking; however, damage in the joint is inevitable due to concrete pry-out failure and pullout of anchored rebars in case of concrete having low strength. The same is also dependent on the quality of epoxy (i.e., anchor-concrete bond) and embedded length of rebars. In present case, the rebars embedded length was based on experimental pullout tests; however, analytical models may be used to select an appropriate development length for embedded rebars.

The model floor displacement was multiplied by a scale factor $S_L = 3.0$ while the base shear force was multiplied by a scale factor $S_L^2 = 3^2$ to obtain the corresponding prototype model response. Figure 9 reports the lateral force-displacement capacity curves of the retrofitted RC frames. Capacity curve of as-built structure tested by Rizwan et al. [19] is also reported. It can be observed that the retrofitted frames have exhibited increase in stiffness and lateral strength in comparison to as-built frame. In case of Model-M_{RC}, the stiffness increased by 120% while the corresponding lateral strength was increased by 20%. In case of Model-M_{RC2}, the stiffness increased by 160% while the corresponding

(a)

(b)

(c)

Figure 7: Observed damage in deficient models retrofitted with RC haunches, scheme-1. (a) Damage observed in columns during 30% run. (b) Damage observed in beam and columns during 40% run. (c) Damage observed in columns, respectively, under 50% and 70% run.

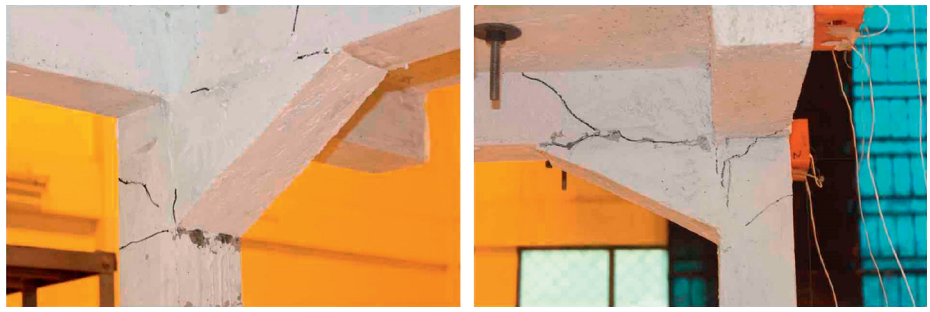

(a)

Figure 8: Continued.

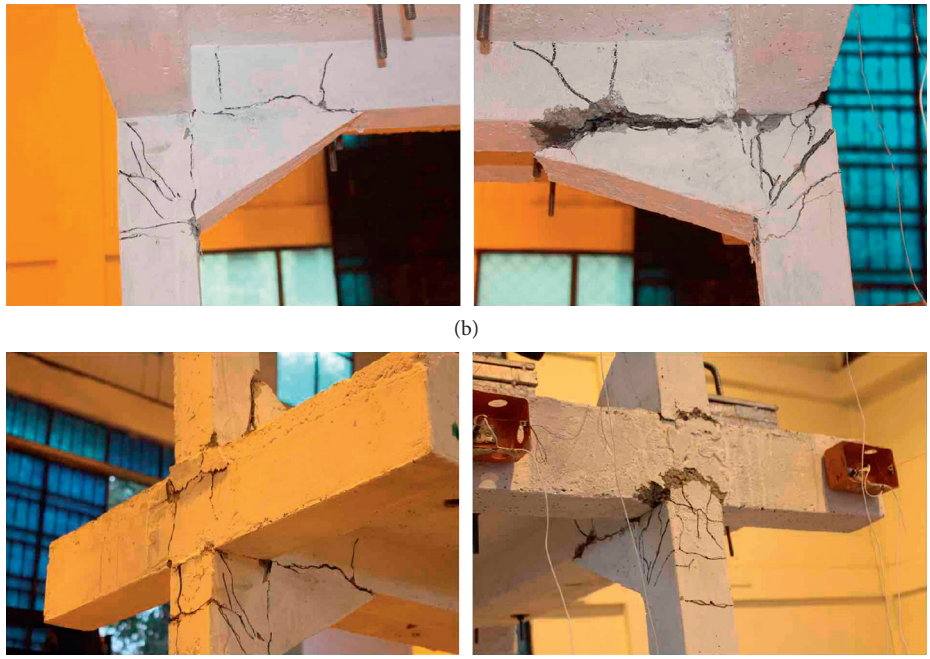

(b)

(c)

Figure 8: Observed damage in deficient models retrofitted with RC haunches, scheme-2. (a) Damage observed in beam-columns connection during self-check run. (b) Damage observed in beam-columns connection during 80% run. (c) Damage observed in beam-columns connection during 80% run.

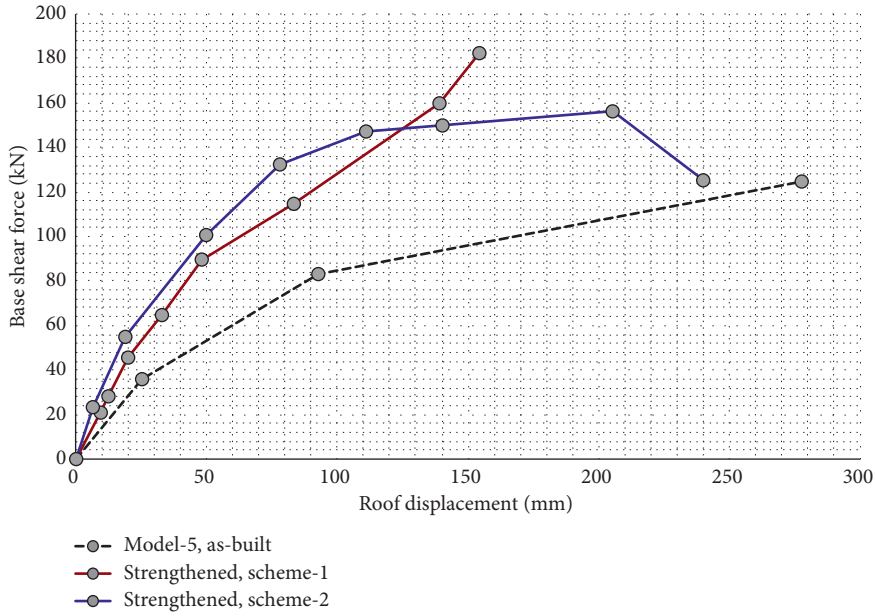

Figure 9: Lateral force-deformation response of as-built and RC haunch retrofitted frames.

lateral strength was increased by 28%. It is worth to mention that the as-built frame deformed to relatively larger displacement in comparison to haunch retrofitted frames; however, the seismic code suggests maximum displacement capacity corresponding to 2.50% drift for calculating global structural ductility. Later, it will be demonstrated that the strengthening also increases the transitional ductility of frame. The increase in stiffness, strength, and ductility indicates increase in the response modification factor of structure.

4. Numerical Modelling of RC Haunch Retrofitted RC Frame

4.1. Calibration of FE-Based Numerical Model. In the present study, inelastic modelling technique proposed and employed earlier by Ahmad et al. [39, 40], for RC frames having weaker beam-column joints retrofitted with steel haunches, was adopted and extended for modelling of RC frames retrofitted with reinforced concrete haunches. The numerical models were prepared in finite element based software SeismoStruct employed for nonlinear static and dynamic seismic analysis [41]. The numerical model comprised fibre-section based flexure elements for modelling beam/column members, inelastic lumped hinges to simulate joint shear hinge, and a rigid link along with inelastic truss element to approximate response of haunches (Figure 10). The RC haunches were applied continuously over a length of 1 h (where h is the depth of section), as shown in Figure 4; these primarily resist the axial compression and tension forces. For this, the numerical model used inelastic truss elements that only resist the axial forces. The width of truss was equal to the width of column (i.e., 12 inches) while the depth = 12 inches was selected through trial analysis. Alternatively, the area of truss can be calculated directly from the axial force developed in the truss member under the lateral loads developing plastic moment capacity in beam.

Inelastic force-based flexure beam-type element with fibre-section was used for modelling of both beam and column members (Figure 11). The fibre-section element uses the finite element formulation [42, 43] to relate the section stress-strain response, which is based on the materials uniaxial stress-strain behaviour, with the element actions (axial, shear, bending) and deformations (displacement, rotations), and able to model both the geometric nonlinearity and material inelasticity of members. It can simulate both the softening and hardening behaviour of beam/column members [44]. Since the flexure capacity of beam/column members was relatively less, and these members were observed with flexure mechanism during shake table tests, the shear modelling for beam/column elements was ignored for simplification of modelling technique.

To model RC beam-column connections, there are different modelling techniques proposed [45–49], most of which work on the concept that moment is transferred through rotational spring simulating joint shear deformation. In the present study, a simplified numerical modelling technique used by Ahmad et al. [39, 40] was adopted, which was extended herein to model the RC frames retrofitted with reinforced concrete haunches. The modelling technique accounts for shear hinging of beam-column joint panel, which is essential for RC frames having weaker panel zone. The technique comprised idealizing beam-column joint panel with a stiff elastic flexure beam-type element, which are provided with zero-length link elements at the centre of joint. This connects the joint horizontal element with the vertical elements through a rotational spring (Figure 12). The longitudinal rebars slip that causes fixed-end rotation at the ends of beam was modelled by introducing a zero-length link-element at the beam ends.

Joint panel is provided with moment-rotation spring, which was assigned with multi-linear constitutive law of Sivaselvan and Reinhorn [51] in order to simulate joint shear nonlinearity. Alath and Kunnath's [45] model proposed for scissor type joint for simulating joint shear was used for calculating rotational spring moment capacity. This basically relates the joint shear with moment capacity of shear-hinge spring based on the equilibrium consideration of connection:

$$M_j = \tau_{jh} A_{jh} \frac{1}{((1 - b/L_b)/jd) - (1 - L_C)}, \quad (1)$$

where $A_{jh} = b_j \times h_j$ represents shear area of the joint, M_j represents moment capacity of the rotational spring, h_j and b_j represent depth and width of joint core respectively, L_c is the total length of column above and below the panel, L_b is the total length of beam on left and right side of joint between the contra-flexure points, j_d is the internal moment arm for the corresponding moment at the beam ends, and τ_{jh} is the joint shear strength corresponding to diagonal tensile strength of joint and between the contra-flexure points. The maximum shear strength of joint was obtained using the analytical model of Priestley [38] and Pampanin et al. [17] for nonseismic joints.

To model rotational capacity of spring for various limits of damage state, the model additionally specifies deformation limits proposed by Magenes and Pampanin [50] for modelling of spring limit state rotational capacity. This is for the purpose of developing the multi-linear constitutive law assigned to moment rotation spring [51], as reported in Figure 13. Experimental studies have shown pinched shear stress-strain behaviour for beam-column joints lacking ties in joints. Peak shear strength of 146 kN was calculated for the joint.

Beam-ends rotation, which contributes to the additional deformations (chord-rotation) of beam member, is caused by longitudinal reinforcement bar-slip and inelastic extension of rebars. Beam-ends link-element provisioned with in-plane moment-rotation spring was used to model the additional deformation of beam member. The spring was assigned with bi-linear constitutive law having post-yielding hardening behaviour, as suggested by Ahmad et al. [40].

4.2. Testing and Validation of the Proposed Numerical Model. A representative prototype model of the tested RC frames was developed using the finite element-based software SeismoStruct (Figure 14) for testing and validation, and subsequent calibration, of the aforementioned modelling technique in predicting the roof displacement response and base shear force. Acceleration time histories recorded at the base of model during experimental testing were applied on respective FE model and its response in the form of roof displacement, base shear, and local damage mechanism was studied.

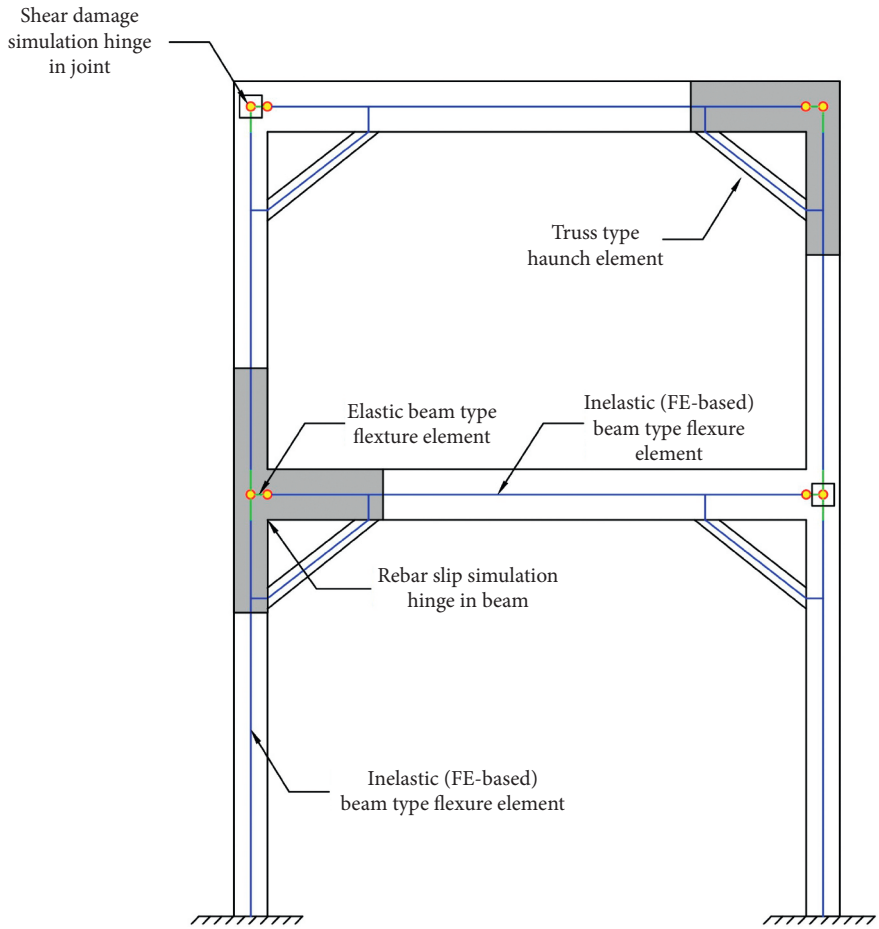

Figure 10: Structural frame idealization; RC frame inelastic modelling after [40].

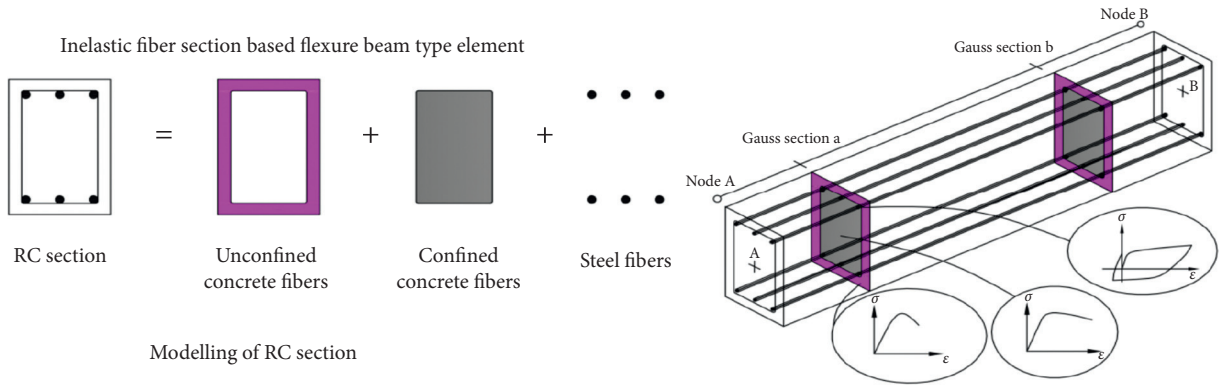

Figure 11: Idealization of beams and columns members, FE based frame element's inelastic modelling.

It is worth mentioning that numerical models always exhibit numerical damping in addition to the elastic and hysteretic damping. Due to this, the total damping of structure increases compared to the actual. Various studies have been carried out that suggest taking lower value of damping from 0% to 2% [52]. In a previous research, the authors have found that taking 2% elastic damping was fair in simulating the time history response of frame displacement. Therefore, elastic damping of 2% was taken, which was assigned to the model using tangent stiffness proportional Rayleigh damping model. Figures 15(a) and 15(b) show the roof lateral displacement response of the structure predicted using SeismoStruct, which was compared with the experimentally observed roof displacement response. The

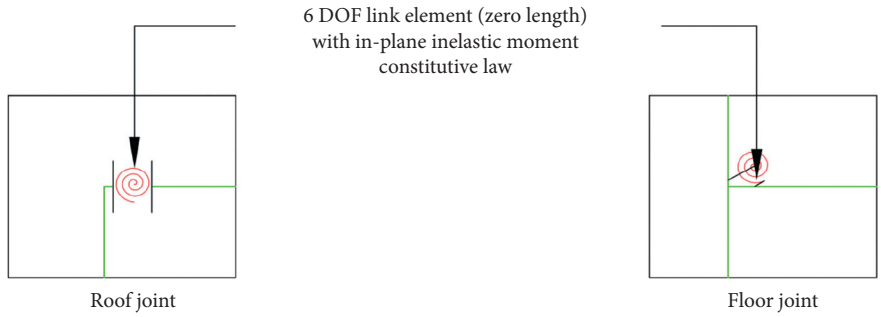

Figure 12: Idealization and modelling of joint shear simulation hinge.

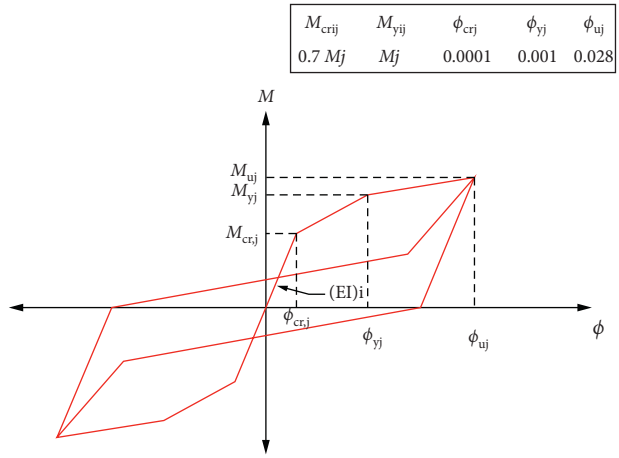

Figure 13: Moment-rotation hysteretic response of spring simulating shear hinge in joints.

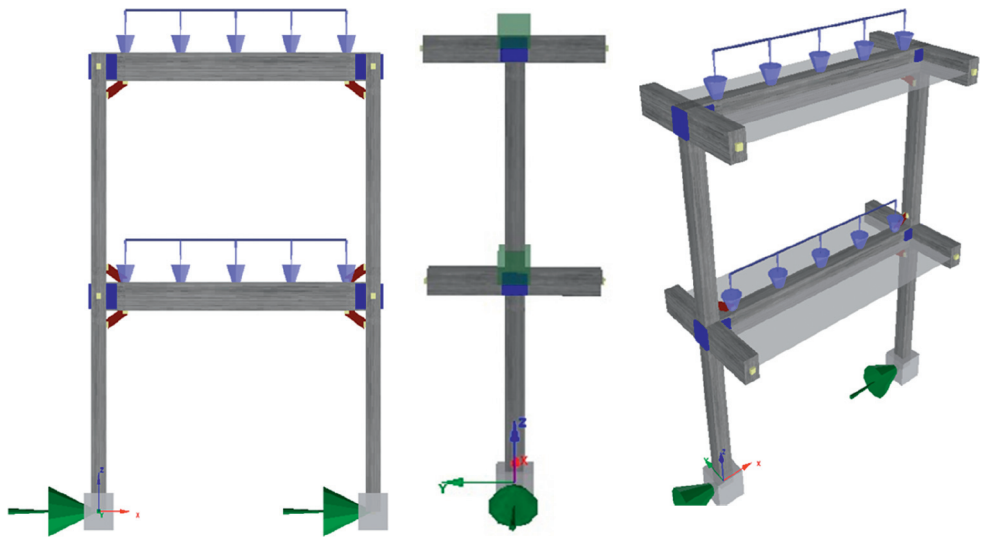

Figure 14: Numerical model of haunch retrofitted RC frame prepared in SeismoStruct.

proposed technique was efficient in predicting the response of model-1 M_{RC}. However, the same technique was found less accurate in case of model-2 M_{RC2}. The numerical model was efficient in predicting the trend of time history response of roof displacement but the numerical model missed predicting the exact peaks. One possible reason seems to be

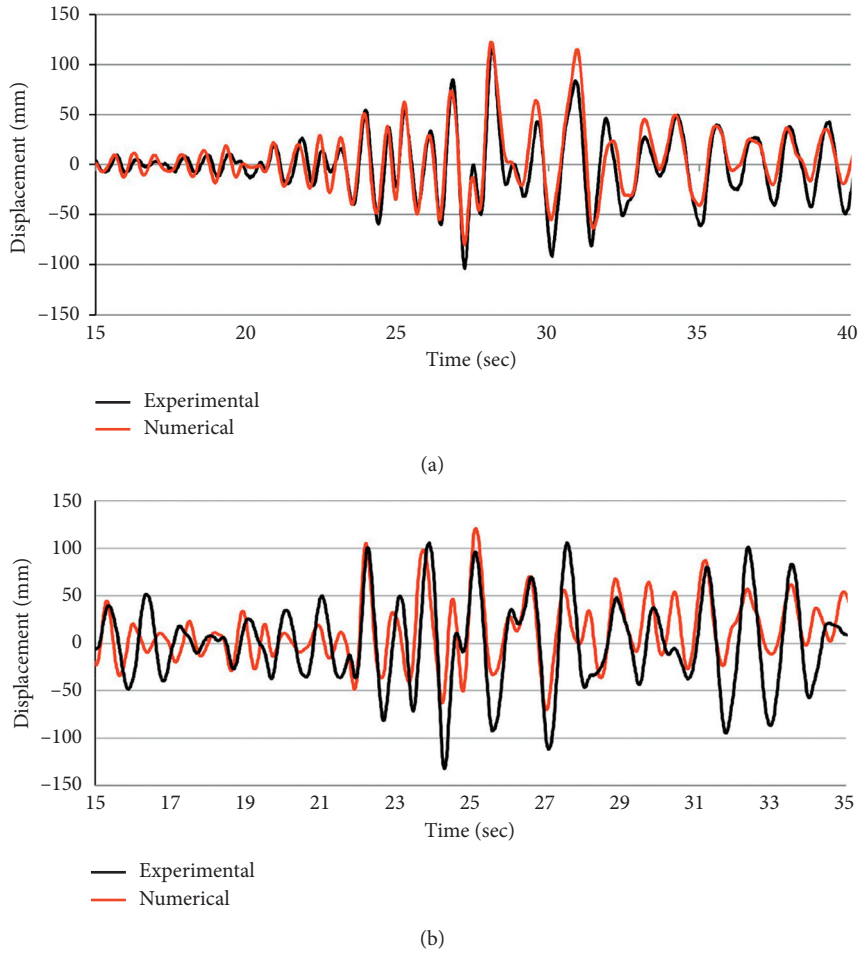

FIGURE 15: Simulation of roof displacement time history response in SeismoStruct. (a) Model-M_{RC} having RC haunch below beam only. (b) Model-M_{RC2} having RC haunches both below and above beam.

the elastic modelling of haunch anchors, which experienced anchors-slip and pullout under strong shaking. This phenomenon was prominent in case of model-2, $M_{RC2,}$ as observed during shake table tests (Figure 8). The error in predicting the peak roof displacement was 1.54% for Model-M_{RC} and 9.06% for Model-M_{RC2}. Similarly, error in predicting peak base shear force was also calculated for each model and was found to be 6.40% for Model-M_{RC} and 4.63% for Model-M_{RC2}.

5. Response Modification Factor

5.1. Based on Experimental Shake Table Tests. The present study included both the analytical and numerical procedures to calculate response modification R factor. The analytical approach involved the derivation of lateral force-deformation capacity curve of models based on the experimental shake table tests, and using the analytical formulae of Newmark and Hall [53] to quantify R. Similar approach has been used in a number of recent studies [19, 54]. By definition, R factor of a structure is the reduction required for reducing elastic base shear force of a structure used for seismic design of structures:

$$R = \frac{V_e}{V_s} = \frac{V_e}{V_s} \cdot \frac{V_e}{V_s} = R_\mu \cdot R_s. \tag{2}$$

Here, V_e is the elastic force demand, V_y is the idealized yield strength, V_s is the design base shear force, $R\mu$ is the ductility factor, and R_S is the overstrength factor. R_S was obtained from lateral force-deformation capacity curve of the structure directly, which is the idealized yield strength divided by the structure design strength. $R\mu$ was calculated using the analytical formulae of Newmark and Hall [53]:

$$\begin{aligned}
&\text{short period: } T < 0.20\text{sec} \quad R_\mu = 1.0,\\
&\text{intermediate period: } 0.2\text{sec} < T < 0.5\text{sec} \quad \sqrt{2_\mu - 1},\\
&\text{long period: } T > 0.5\text{sec} \quad R_\mu = \mu,\\
&\text{structure vibration period:} \quad T = 2\pi\sqrt{\frac{m}{k_y}},
\end{aligned} \tag{3}$$

where T is the pre-yield vibration period of idealized single degree of freedom (SDOF) system and μ is the ductility ratio.

For this purpose, the experimentally derived capacity curves were bi-linearized using the energy-balance criterion; i.e., the area under the idealized force-displacement capacity curve is equal to the area under the curve of the actual force-displacement response. Figure 16 shows the bilinearization idealization while Figure 17 shows the obtained elastoplastic capacity curves for both as-built and retrofitted RC frames.

The classical vibration period formula was used for calculating structure vibration period, which was greater than 0.50 sec. The ultimate displacement capacity of model was based on the minimum of the allowable story drift capacity of structure given in code or the displacement capacity corresponding to the life safety (LS) drift limit of structure. The Building Code of Pakistan [55] suggests story drift of 2.50% for the considered low-rise structures. This corresponds to a displacement capacity of 7.20 inches (183 mm). The displacement capacity corresponding to the LS limit states was computed in accordance with the FEMA 356 [56], i.e., $\text{Drfit}_{\text{LS}} = 0.75\ \text{Drift}_{\text{CP}}$, where Drfit_{LS} is the drift corresponding to life safety performance level and Drift_{CP} is the drift corresponding to the near collapse state. The ultimate displacement capacity was divided by the idealized yield displacement to calculate the ductility ratio μ, which in the present case is equal to the ductility factor $R\mu$. The ductility factor $R\mu$ was multiplied with the overstrength factor R_S to quantify the response modification factor R. The calculated seismic response parameters are shown in Figure 18. The calculated R factor for as-built frame was found to be 2.90 ($R = 3.0$, approx.). In case of RC retrofitted frames, the calculated R factor increased to 4.09 ($R = 4.0$, appox.) in case of Model-M_{RC} and 7.76 ($R = 7.50$, approx.) in case of Model-M_{RC2} (Figure 18). This indicates an increase of 41% and 167% using RC haunches just below the beam and both below and above the beam, respectively.

5.2. Based on Incremental Dynamic Analysis (IDA) of Numerical Models. The seismic response modification factor R calculated experimentally is dependent upon the capacity curve derived for a single and specific accelerogram through shake table testing on model structure. Also, the analytical models developed earlier are based on calculations in which the energy dissipation for the considered structure is not clearly taken into account. Therefore, a numerical model (discussed above in detail) was also analyzed for calculation of R factor. This will enable taking into account the variability in structure response due to differences in ground motions and also taking into account the actual energy dissipation capacity of the structure. For this purpose, structure response and seismic capacity curves were derived using the incremental dynamic analysis (IDA) procedure employing different natural acceleration time histories.

The PEER NGA strong ground motion database was used to retrieve a suite of seven accelerograms (Table 1), for this search criterion was prespecified to meet the regional tectonics of Pakistan for high hazard zones. The tectonic parameters considered from NGA-West 2 ground motion were the following: moment magnitude M_W was from 6.0 to 8.0, the considered soil type was stiff "type B" having VS_{30} from 500 m/sec to 750 m/sec, the closest distance to fault rupture R_{jb} and R_{rup} was from 10 km to 30 km, and faults mechanism was considered to be reverse/oblique. Each accelerogram retrieved from the database was analyzed very carefully for selection, considering region-to-region and event-to-event variability. Wavelet-based approach employed in Seismo-Match was used for scaling and matching of the selected accelerograms to the design spectrum for seismic zone 4 having design PGA = 0.40 g (Figure 19).

The IDA procedure was used to derive the structural capacity and response curves by subjecting the numerical models to all the selected accelerograms. The matched acceleration time histories were linearly scaled to multiple levels of PGA. The capacity curves were obtained by relating the obtained peak demand in each run with the respective base shear force while the seismic response curves were obtained by relating the peak drift obtained in each run with the corresponding PGA. The capacity curves were analyzed for identifying the yielding point, and the overstrength R_s was calculated as the ratio of the lateral resistance corresponding to yielding to the design base shear. The ductility factor $R\mu$ was calculated by analyzing the seismic response curves, which is equal to the ratio of PGA at ultimate drift limit to the seismic intensity corresponding to the idealized yielding displacement of the model [57, 58]:

$$R_{\mu} = \frac{\text{PGA}_{\Delta,\text{Ultimate}}}{\text{PGA}_{\Delta,\text{Yield}}}. \tag{4}$$

The ultimate displacement capacity corresponds to the code allowed drift capacity of 2.50% for low-rise structures. Other recent studies have also adopted the above approach to calculate the ductility factor [54, 59–62]. The calculation of R as an example for a single earthquake record for Model-M_{RC} is shown in Figure 20. In the same way, R was calculated for other selected earthquake records for the same model and for Model-M_{RC2}. An average value of 4.03 and 7.75 was obtained for Model-M_{RC} and Model-M_{RC2}, respectively.

6. Seismic Performance Assessment of As-Built and Retrofitted Frames

Most of the seismic codes suggest static force-based procedure for the seismic analysis and design of structures. The BCP [55], which is based on the UBC-97, included equations for calculating base shear force:

$$V = C_S \times W, \tag{5}$$

where

$$C_S = \frac{C_V I}{RT}. \tag{6}$$

However, it should not be greater than the maximum allowed:

$$C_{S,max} = \frac{2.5C_a}{R}, \tag{7}$$

where W = weight of the structure, C_S = base shear coefficient, I = importance factor, R = response modification factor, and C_a and C_V = seismic coefficients for seismic zone.

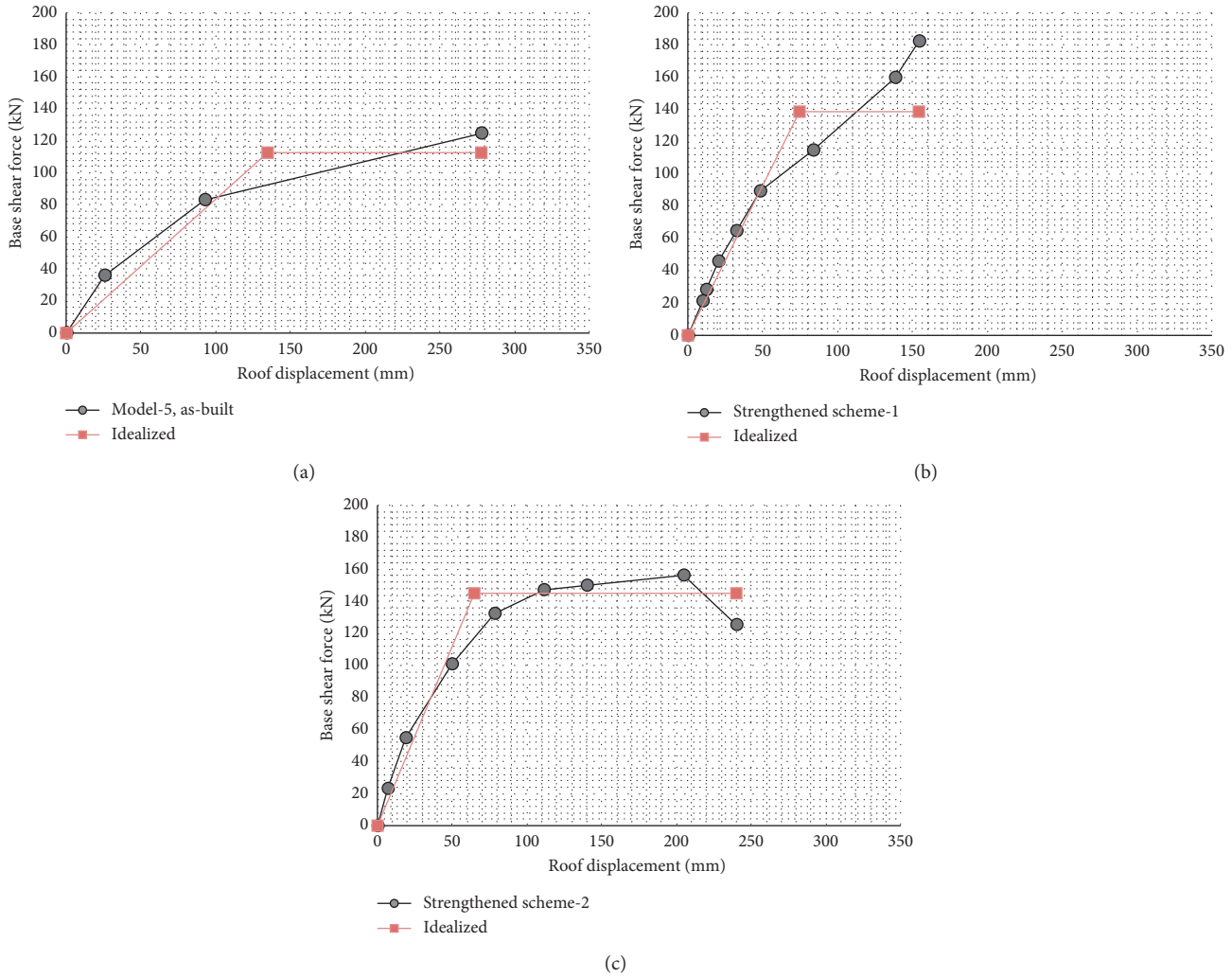

Figure 16: Bilinear idealizations of force-displacement capacity curves. (a) Model-5, as-built [19]. (b) Retrofitted, scheme-1. (c) Retrofitted, scheme-2. Elastoplastic idealization of capacity curves. First, the maximum displacement capacity of models was identified. The yield force and yield displacement were varied to equalize the area under the elastoplastic curve to that of actual curve. The yield stiffness was checked not to vary much in comparison to initial stiffness.

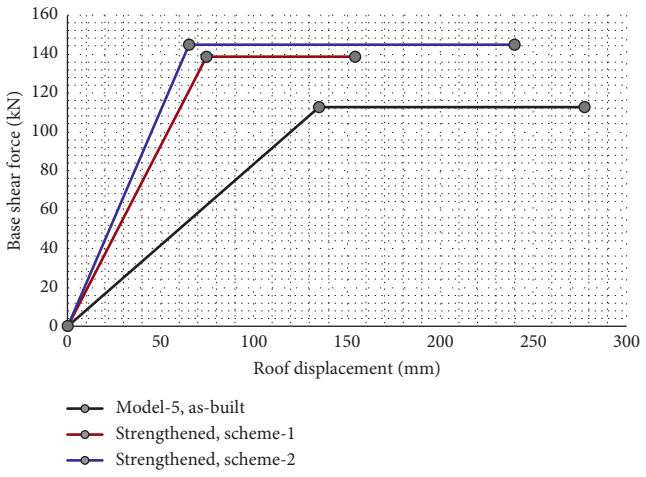

Figure 17: Bilinearized lateral force-deformation response of as-built and retrofitted RC frames.

Equations (5)–(7) were used to calculate seismic design base shear force for both the as-built and retrofitted structure for various seismic zones: 1, 2A, 2B, 3 and 4, and site soil type B "rock." For as-built RC frame, R factor of 3.0 was considered while an average value of R factor 7.50 was considered for the retrofitted frame, considering that frame is retrofitted with RC haunches applied both below and above the beam. The demand on structures was calculated in terms of base shear coefficient (C_S, Demand), which was compared with the design level base shear coefficient (C_S, Capacity) of the structures. C_S, Capacity is the design level base shear coefficient for which the considered frames were designed. Tables 2 and 3 report the factor of safety (FoS) for both the as-built and retrofitted frames. It can be observed that the as-built RC frame can perform better in all seismic zones; however, the structure will not be able to perform better in seismic zones 3 and 4. On the other hand, the haunch-retrofitted frames can perform satisfactorily in all seismic zones with significantly higher factor of safety.

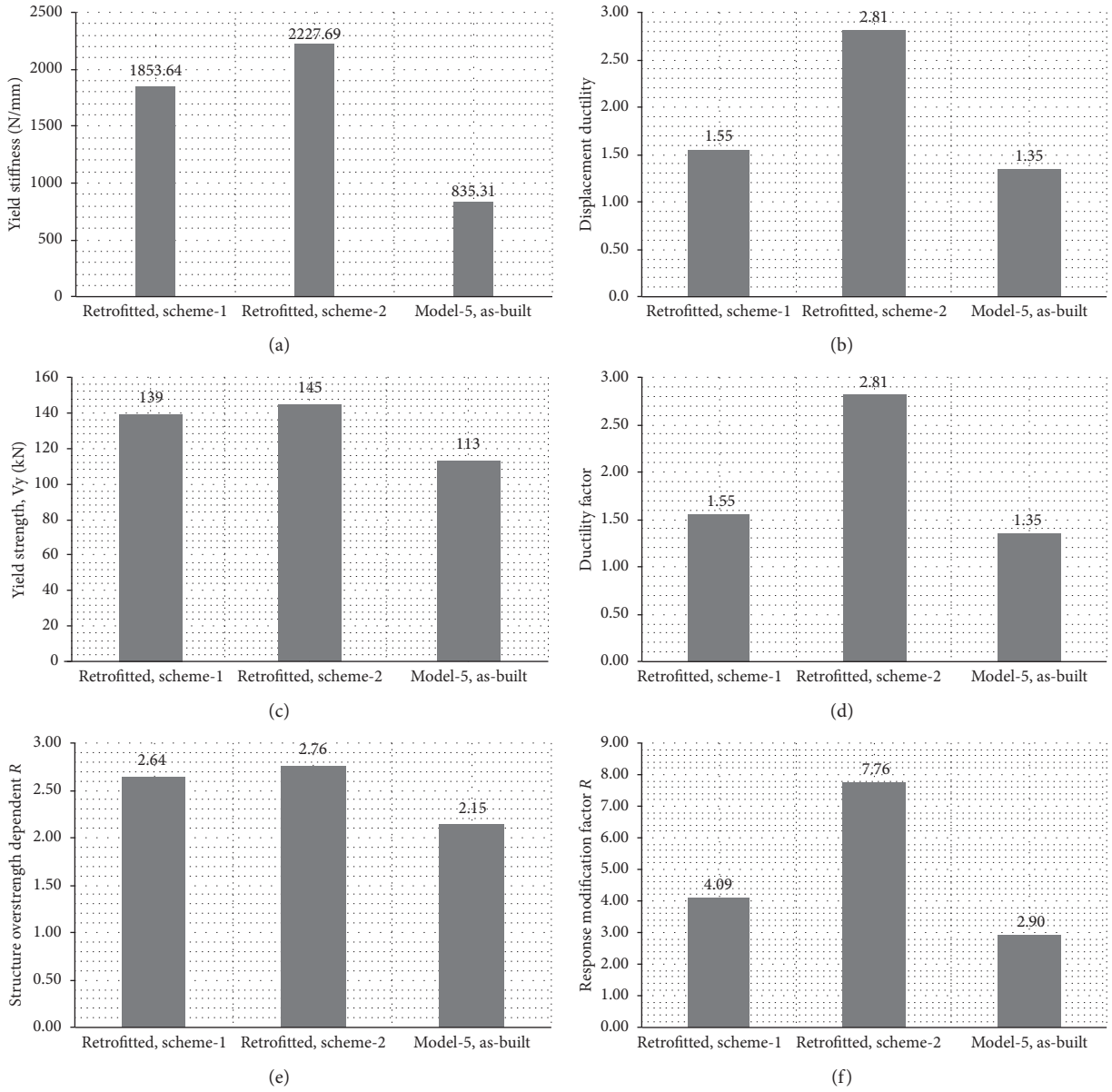

Figure 18: Seismic response parameters of as-built and strengthened RC frames obtained experimentally. (a) Yield stiffness. (b) Structure ductility. (c) Yield strength. (d) Ductility factor, $R\mu$. (e) Overstrength factor, Ω_0. (f) Response modification factor, R.

Table 1: Details of selected acceleration time histories for incremental dynamic analysis.

Record no.	Year	Event	Station/component	Moment magnitude (Mw)	Matched PGA (g)
1	1999	Duzce Turkey	Bolu	7.14	0.418
2	1989	Loma Prieta	Hollister-South & Pine	6.93	0.24
3	1995	Kobe Japan	Abeno	6.90	0.327
4	1988	Spitak Armenia	Gukasian	6.77	0.300
5	1971	San Fernando	LA-Hollywood Stor FF	6.61	0.346
6	1979	Imperial Valley-06	El-Centro Array #12	6.53	0.291
7	1980	Victoria, Mexico	Chihuahua	6.33	0.235

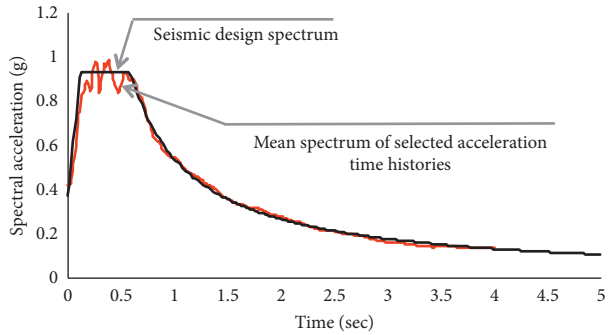

Figure 19: Comparison of mean spectrum of matched acceleration records to the seismic design spectrum.

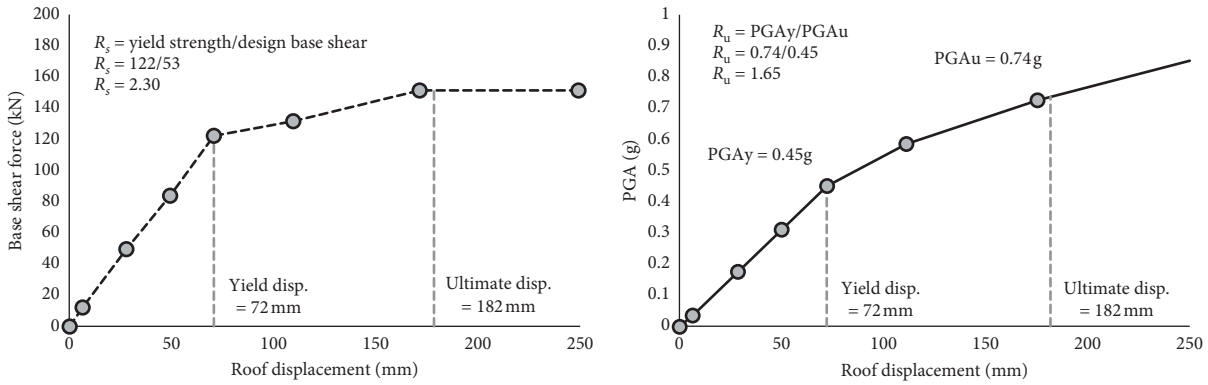

Figure 20: Calculation of R factor based on the IDA analysis, $R = R_s \times R_\mu = 3.80$. An example for Model-$M_{RC}$ for Kobe accelerogram. (a) IDA-based capacity curve. (b) IDA-based response curve.

Table 2: Seismic performance of as-built RC frame in various seismic zones.

Zone	C_a	C_V	Cs, demand ($R = 3.0$)	Cs, capacity	FoS	Remarks
1	0.08	0.08	0.06		3.45	OK
2A	0.15	0.15	0.11		1.84	OK
2B	0.2	0.2	0.14	0.20	1.38	OK
3	0.3	0.3	0.22		0.92	N.G.
4	0.4	0.4	0.29		0.69	N.G.

Table 3: Seismic performance of haunch retrofitted RC frame in various seismic zones.

Zone	C_a	C_V	Cs, demand ($R = 7.50$)	Cs, capacity	FoS	Remarks
1	0.08	0.08	0.03		7.88	OK
2A	0.15	0.15	0.05		4.20	OK
2B	0.2	0.2	0.06	0.20	3.15	OK
3	0.3	0.3	0.10		2.10	OK
4	0.4	0.4	0.13		1.58	OK

7. Conclusions and Recommendations

The following conclusions were drawn on the basis of experimental shake table tests performed on as-built and retrofitted RC frames with reinforced concrete haunches:

Noncompliant RC frame incorporating construction deficiencies, i.e., having concrete with low compressive strength, beam/column members having reduced longitudinal and transverse reinforcements, and joints lacking lateral ties, was observed with extensive damage in beam-column joints and columns. This reduced the lateral strength and ductility ratio of RC frames. The overstrength factor Ω_0 was found equal to 2.15 and ductility factor $R\mu$ was found equal to 1.35. This indicates a reduction of 23% and 56% in overstrength and ductility factors, respectively, in comparison to the values suggested in the Building Code of Pakistan.

The application of reinforced concrete haunches at the beam-column connections increased the stiffness and lateral strength of structure and altered the damage mechanism. However, due to the intentional simplicity involved in the haunch installation and low strength of structural concrete, the haunches detached from the beam/column members under extreme shaking. This was followed by cracking in joint panels. Nevertheless, the technique significantly increased the structural stiffness and strength. Although the technique reduced the structural deformability due to stiffening effect of the retrofitting technique, the structural ductility was increased considering the ultimate deformation corresponding to the LS performance level or drift limit given in the seismic code. The increase in the structural

seismic response parameters indicates enhancement in the structural performance against frequent and rare earthquakes.

The retrofitting increased the overstrength factor to 2.64 and 2.76 in case of reinforced concrete haunch applied only below and both below and above the beam, respectively. Similarly, the ductility was increased to 1.55 and 2.81, respectively. The enhancement in overstrength and ductility increased response modification factor of retrofitted frame to 4.09 and 7.76 in case of RC frame retrofitted with RC haunches applied only below the beam and RC haunches applied both below and above the beam, respectively. Haunches installed both below and above the beam performed relatively better than haunches provided below the beam only.

The following conclusions were drawn on the basis of numerical analysis performed on as-built and retrofitted RC frames with reinforced concrete haunches:

The finite element based model developed by authors for deficient RC frames retrofitted with steel haunches was extended for numerical modelling of deficient RC frames retrofitted with reinforced concrete haunches. Since anchors pullout was observed under extreme displacement demand and also this did not cause any substantial decrease in the lateral force carrying capacity of the model, the anchors in numerical models were considered intact throughout the loading. The truss idealization reinforced concrete haunch was considered as an inelastic axial element. The cross section of truss element was approximated as rectangular with width equal to the width of column. The depth of section was selected after trial analysis. Section with depth of 12 inches (305 mm) provided relatively better result in simulating time history of response displacement, peak displacement, and peak force.

The proposed technique was efficient in predicting the response of model-1 M_{RC}, in case haunches when applied only below the beam. However, the same technique was found less accurate in case of model-2 M_{RC2}, in case when haunches were applied both below and above the beams. The numerical model was efficient in predicting the trend of time history response of roof displacement. But, the numerical model missed predicting the exact peaks. One possible reason seems to be the elastic modelling of haunch anchors, which experienced anchors' slip. However, the error in predicting the peak roof displacement was 1.54% for Model-M_{RC} and 9.06% for Model-M_{RC2}. Similarly, error in predicting peak base shear force was also calculated for each model and was found to be 6.40% for Model-M_{RC} and 4.63% for Model-M_{RC2}. This seems to be reasonable for global assessment of structures for quantification of response modification factor.

The numerically calculated response modification factor was found reasonably in good agreement with the experimentally/analytically calculated response modification factor. Slight difference was due to the variability in ground motions.

The following conclusions were drawn on the basis of static force procedure used for seismic performance assessment of as-built and retrofitted RC frames with reinforced concrete haunches:

Noncompliant RC frame was only able to perform better in low-to-moderate seismic zones (i.e., zones 1, 2A, 2B); however, the structure was found "No Good" in the seismic zones 3 and 4.

The retrofitted RC frame was found "OK" in all seismic zones, indicating beneficial role of local retrofit in improving global seismic performance of structure.

Data Availability

All data, models, or codes generated or used during the study are available from the corresponding author upon request (Naveed Ahmad, naveed.ahmad@uetpeshawar.edu.pk). Items that may be requested are as follows: shake table tests data of both as-built and retrofitted models (raw and processed data) and SeismoStruct numerical models.

Conflicts of Interest

The authors declare that they have no conflicts of interest.

References

[1] S. Ates, V. Kahya, M. Yurdakul, and S. Adanur, "Damages on reinforced concrete buildings due to consecutive earthquakes in Van," *Soil Dynamics and Earthquake Engineering*, vol. 53, pp. 109–118, 2013.

[2] L. E. Aycardi, J. B. Mander, and A. M. Reinhorn, "Seismic resistance of reinforced concrete frame structures designed only for gravity loads: experimental performance of subassemblages," *ACI Structural Journal*, vol. 91, no. 5, pp. 552–563, 1994.

[3] İ. E. Bal, H. Crowley, R. Pinho, and F. G. Gülay, "Detailed assessment of structural characteristics of Turkish RC building stock for loss assessment models," *Soil Dynamics and Earthquake Engineering*, vol. 28, no. 10-11, pp. 914–932, 2008.

[4] A. Beres, S. P. Pessiki, R. N. White, and P. Gergely, "Implications of experiments on the seismic behavior of gravity load designed RC beam-to-column connections," *Earthquake Spectra*, vol. 12, no. 2, pp. 185–198, 1996.

[5] J. K. Bothara and K. M. O. Hiçyılmaz, "General observations of building behaviour during the 8th October 2005 Pakistan earthquake," *Bulletin of the New Zealand Society for Earthquake Engineering*, vol. 41, no. 4, pp. 209–233, 2008.

[6] J. M. Bracci, A. M. Reinhorn, and J. B. Mander, "Seismic resistance of reinforced concrete frame structures designed for gravity loads: performance of structural system," *ACI Structure Journal*, vol. 92, no. 5, pp. 597–609, 1995a.

[7] H. Chaulagain, H. Rodrigues, E. Spacone, and H. Varum, "Seismic response of current RC buildings in Kathmandu Valley," *Structural Engineering and Mechanics*, vol. 53, no. 4, pp. 791–818, 2015.

[8] S. Doocy, A. Daniels, C. Packer, A. Dick, and T. D. Kirsch, "The human impact of earthquakes: a historical review of events 1980–2009 and systematic literature review," *PLoS Currents*, vol. 1, 2013.

[9] B. Erdil, "Why RC buildings failed in the 2011 Van, Turkey, earthquakes: construction versus design practices," *Journal of*

Performance of Constructed Facilities, vol. 31, no. 3, Article ID 04016110, 2016.

[10] S. Hakuto, R. Park, and H. Tanaka, "Seismic load tests on interior and exterior beam-column joints with substandard reinforcing details," *ACI Structural Journal*, vol. 97, no. 1, pp. 11–25, 2000.

[11] S. A. Khan, K. Pilakoutas, I. Hajirasouliha, R. Garcia, and M. Guadagnini, "Seismic risk assessment for developing countries: Pakistan as a case study," *Earthquake Engineering and Engineering Vibration*, vol. 17, no. 4, pp. 787–804, 2018.

[12] J. G. Ruiz-Pinilla, J. M. Adam, R. Pérez-Cárcel, J. Yuste, and J. J. Moragues, "Learning from RC building structures damaged by the earthquake in Lorca, Spain, in 2011," *Engineering Failure Analysis*, vol. 68, pp. 76–86, 2016.

[13] J. Shafaei, A. Hosseini, M. S. Marefat, J. M. Ingham, and H. Zare, "Experimental evaluation of seismically and non-seismically detailed external RC beam-column joints," *Journal of Earthquake Engineering*, vol. 21, no. 5, pp. 776–807, 2017.

[14] S. Yavari, K. J. Elwood, C. L. Wu, S. H. Lin, S. J. Hwang, and J. P. Moehle, "Shaking table tests on reinforced concrete frames without seismic detailing," *ACI Structural Journal*, vol. 110, no. 06, pp. 1000–1012, 2013.

[15] N. Ahmad, A. Shahzad, M. Rizwan et al., "Seismic performance assessment of non-compliant SMRF-reinforced concrete frame: shake-table test study," *Journal of Earthquake Engineering*, vol. 23, no. 3, pp. 444–462, 2019a.

[16] G. M. Calvi, G. Magenes, and S. Pampanin, "Relevance of beam-column joint damage and collapse in RC frame assessment," *Journal of Earthquake Engineering*, vol. 6, no. sup1, pp. 75–100, 2002.

[17] S. Pampanin, G. M. Calvi, and M. Moratti, "Seismic behavior of R.C. beam-column joints designed for gravity only," in *Proceedings of the 12th European Conference on Earthquake Engineering*, Barbican Centre, London, UK, September 2002.

[18] R. Park, "A summary of results of simulated seismic load tests on reinforced concrete beam-column joints, beams and columns with substandard reinforcing details," *Journal of Earthquake Engineering*, vol. 6, no. 2, pp. 1–27, 2002.

[19] M. Rizwan, N. Ahmad, and A. N. Khan, "Seismic performance of compliant and non-compliant special moment-resisting Reinforced Concrete Frames," *ACI Structural Journal*, vol. 115, no. 4, 2018.

[20] M. Rizwan, N. Ahmad, A. Naeem Khan, S. Qazi, J. Akbar, and M. Fahad, "Shake table investigations on code non-compliant reinforced concrete frames," *Alexandria Engineering Journal*, vol. 59, no. 1, pp. 349–367, 2020.

[21] A. Sharma, G. R. Reddy, and K. K. Vaze, "Shake table tests on a non-seismically detailed RC frame structure," *Structural Engineering and Mechanics*, vol. 41, no. 1, pp. 1–24, 2012.

[22] A. Benavent-Climent, L. Morillas, and D. Escolano-Margarit, "Seismic performance and damage evaluation of a reinforced concrete frame with hysteretic dampers through shake-table tests," *Earthquake Engineering & Structural Dynamics*, vol. 43, no. 15, pp. 2399–2417, 2014.

[23] J. Bracci, A. Reinhorn, and J. Mander, "Seismic retrofit of reinforced concrete buildings designed for gravity loads: performance of structural model," *ACI Structural Journal*, vol. 92, no. 6, pp. 711–723, 1995b.

[24] M. Dolce, D. Cardone, and F. C. Ponzo, "Shaking-table tests on reinforced concrete frames with different isolation systems," *Earthquake Engineering & Structural Dynamics*, vol. 36, no. 5, pp. 573–596, 2007.

[25] M. Dolce, D. Cardone, F. C. Ponzo, and C. Valente, "Shaking table tests on reinforced concrete frames without and with passive control systems," *Earthquake Engineering & Structural Dynamics*, vol. 34, no. 14, pp. 1687–1717, 2005.

[26] M. Engindeniz, L. F. Kahn, and A. H. Zureick, "Repair and strengthening of reinforced concrete beam-column joints: state of the art," *ACI Structural Journal*, vol. 102, no. 2, 2005.

[27] R. Garcia, I. Hajirasouliha, and K. Pilakoutas, "Seismic behaviour of deficient RC frames strengthened with CFRP composites," *Engineering Structures*, vol. 32, no. 10, pp. 3075–3085, 2010.

[28] A. Ghobarah and A. Said, "Seismic rehabilitation of beam-column joints using FRP laminates," *Journal of Earthquake Engineering*, vol. 5, no. 1, pp. 113–129, 2001.

[29] X. Lu, B. Yang, and B. Zhao, "Shake-table testing of a self-centering precast reinforced concrete frame with shear walls," *Earthquake Engineering and Engineering Vibration*, vol. 17, no. 2, pp. 221–233, 2018.

[30] M. R. Shiravand, A. K. Nejad, and M. H. Bayanifar, "Seismic response of RC structures rehabilitated with SMA under near-field earthquakes," *Structural Engineering and Mechanics*, vol. 63, no. 4, pp. 497–507, 2017.

[31] F. Zhou and P. Tan, "Recent progress and application on seismic isolation energy dissipation and control for structures in China," *Earthquake Engineering and Engineering Vibration*, vol. 17, no. 1, pp. 19–27, 2018.

[32] J. Akbar, N. Ahmad, B. Alam, and M. Ashraf, "Seismic performance of RC frames retrofitted with haunch technique," *Structural Engineering and Mechanics*, vol. 67, no. 1, pp. 1–8, 2018.

[33] S. Pampanin, C. Christopoulos, and T.-H. Chen, "Development and validation of a metallic haunch seismic retrofit solution for existing under-designed RC frame buildings," *Earthquake Engineering & Structural Dynamics*, vol. 35, no. 14, pp. 1739–1766, 2006.

[34] A. Sharma, G. R. Reddy, R. Eligehausen, G. Genesio, and S. Pampanin, "Seismic response of reinforced concrete frames with haunch retrofit solution," *ACI Structural Journal*, vol. 111, no. 3, pp. 673–684, 2014.

[35] B. Wang, S. Zhu, Y.-L. Xu, and H. Jiang, "Seismic retrofitting of non-seismically designed RC beam-column joints using buckling-restrained haunches: design and analysis," *Journal of Earthquake Engineering*, vol. 22, no. 7, pp. 1188–1208, 2017.

[36] ACI-318, *ACI 318-05: Building Code Requirements for Structural Concrete*, American Concrete Institute (ACI), Farmington Hills, MI, USA, 2005.

[37] P. Quintana-Gallo, S. Pampanin, A. J. Carr, and P. Bonelli, ""Shake table tests of under designed RC frames for the seismic retrofit of buildings – design and similitude requirements of the benchmark specimen"," in *Proceedings of the New Zealand Society of Earthquake Engineering*, Wellington, New Zealand, 2010.

[38] M. J. N. Priestley, "Displacement-based seismic assessment of reinforced concrete buildings," *Journal of Earthquake Engineering*, vol. 1, no. 1, pp. 157–192, 1997.

[39] N. Ahmad, J. Akbar, M. Rizwan, B. Alam, A. N. Khan, and A. Lateef, "Haunch retrofitting technique for seismic upgrading deficient RC frames," *Bulletin of Earthquake Engineering*, vol. 17, no. 7, pp. 3895–3932, 2019b.

[40] N. Ahmad, A. Shahzad, Q. Ali, M. Rizwan, and A. N. Khan, "Seismic fragility functions for code compliant and non-compliant RC SMRF structures in Pakistan," *Bulletin of Earthquake Engineering*, vol. 16, no. 10, pp. 4675–4703, 2018.

[41] R. Pinho, "Nonlinear dynamic analysis of structures subjected to seismic actions," in *Advanced Earthquake Engineering*

Analysis, A. Pecker, Ed., Springer, Berlin, Germany, pp. 63–89, 2007.

[42] A. Neuenhofer and F. C. Filippou, "Evaluation of nonlinear frame finite-element models," *Journal of Structural Engineering*, vol. 123, no. 7, pp. 958–966, 1997.

[43] E. Spacone, V. Ciampi, and F. C. Filippou, "Mixed formulation of nonlinear beam finite element," *Computers & Structures*, vol. 58, no. 1, pp. 71–83, 1996.

[44] A. Calabrese, J. P. Almeida, and R. Pinho, "Numerical issues in distributed inelasticity modeling of RC frame elements for seismic analysis," *Journal of Earthquake Engineering*, vol. 14, no. sup1, pp. 38–68, 2010.

[45] S. Alath and S. K. Kunnath, "Modeling inelastic shear deformations in RC beam-column joints," in *Proceedings of the Engineering Mechanics 10th Conference*, Boulder, Colorado, May 1995.

[46] A. Biddah and A. Ghobarah, "Modelling of shear deformation and bond slip in reinforced concrete joints," *Structural Engineering and Mechanics*, vol. 7, no. 4, pp. 413–432, 1999.

[47] O. C. Celik and B. R. Ellingwood, "Modeling beam-column joints in fragility assessment of gravity load designed reinforced concrete frames," *Journal of Earthquake Engineering*, vol. 12, no. 3, pp. 357–381, 2008.

[48] L. N. Lowes and A. Altoontash, "Modeling reinforced-concrete beam-column joints subjected to cyclic loading," *Journal of Structural Engineering*, vol. 129, no. 12, pp. 1686–1697, 2003.

[49] M. Youssef and A. Ghobarah, "Modelling of RC beam-column joints and structural walls," *Journal of Earthquake Engineering*, vol. 5, no. 1, pp. 93–111, 2001.

[50] G. Magenes and S. Pampanin, "Seismic response of gravity-load design frames with masonry infills," in *roceedings of the Thirteenth World Conference on Earthquake Engineering*, Vancouver, Canada, August 2004.

[51] M. Sivaselvan and A. M. Reinhorn, "Hysteretic models for deteriorating inelastic structures," *Journal of Engineering Mechanics, ASCE*, vol. 126, no. 6, pp. 633–640, 2001.

[52] L. Petrini, C. Maggi, M. J. N. Priestley, and G. M. Calvi, "Experimental verification of viscous damping modeling for inelastic time history analyzes," *Journal of Earthquake Engineering*, vol. 12, no. sup1, pp. 125–145, 2008.

[53] N. M. Newmark and W. J. Hall, *Earthquake Spectra and Design*, EERI Monograph Series, Earthquake Engineering Research Institute (EERI), Oakland, CA, USA, 1982.

[54] N. Ahmad, Q. Ali, and M. Javed, "Force reduction factor R for shear dominated low-rise brick masonry structures," *Journal of Numerical Methods in Civil Engineering*, vol. 2, no. 3, pp. 14–29, 2019c.

[55] BCP, *Building Code of Pakistan: Seismic Provisions-2007*, Ministry of Housing and Works, Islamabad, Pakistan, 2007.

[56] FEMA 356, *Prestandard and Commentary for the Seismic Rehabilitation of Buildings*, Federal Emergency Management Agency (FEMA), Washington DC, 2000.

[57] A. S. Elnashai and L. Di-Sarno, *Fundamentals of Earthquake Engineering*, John Wiley & Sons, West Sussex, UK, 2008.

[58] A. M. Mwafy and A. S. Elnashai, "Calibration of force reduction factors of RC buildings," *Journal of Earthquake Engineering*, vol. 6, no. 2, pp. 239–273, 2002.

[59] Q. Ali, A. N. Khan, M. Ashraf et al., "Seismic performance of stone masonry buildings used in the Himalayan Belt," *Earthquake Spectra*, vol. 29, no. 4, pp. 1159–1181, 2013.

[60] Q. Ali, T. Schacher, M. Ashraf et al., "In-plane behavior of the dhajji-dewari structural system (wooden braced frame with masonry infill)," *Earthquake Spectra*, vol. 28, no. 3, pp. 835–858, 2012.

[61] A. J. Kappos, "Analytical prediction of the collapse earthquake for R/C buildings: suggested methodology," *Earthquake Engineering & Structural Dynamics*, vol. 20, no. 2, pp. 167–176, 1991.

[62] A. J. Kappos, "Evaluation of behaviour factors on the basis of ductility and overstrength studies," *Engineering Structures*, vol. 21, no. 9, pp. 823–835, 1999.